Running Head: LATE JURASSIC PALEOGEOGRAPHY AND PALEOCLIMATE IN NORTHERN IBERIAN BASIN

LATE JURASSIC PALEOGEOGRAPHY AND PALEOCLIMATE IN THE NORTHERN IBERIAN BASIN OF SPAIN: CONSTRAINTS FROM DIAGENETIC RECORDS IN REEFAL AND CONTINENTAL CARBONATES

M. ISABEL BENITO[1], KYGER C. LOHMANN[2], AND RAMÓN MAS[1]

[1]Dpto. Estratigrafía-U.E.I. de Correlaciones Estratigráficas, Facultad C.C. Geológicas, Universidad Complutense de Madrid-CSIC, 28040 Madrid, Spain

maribel@geo.ucm.es

[2]Department of Geological Sciences, The University of Michigan, Ann Arbor, Michigan 48109-1063, U.S.A. kacey@umich.edu

Key Words: Meteoric diagenesis, isotopes, paleogeography, paleoclimate, Iberian Basin

Manuscript received: Sep 10 2003

ABSTRACT

Sedimentation in the northern part of the Iberian Basin during the early Kimmeridgian was characterized by the development of coral reef complexes of the Torrecilla en Cameros Formation, which were situated along a seaway that connected the Boreal and Tethys Domains. Along the northern portion of that seaway, close to the Boreal Sea, early diagenesis of the Torrecilla fringing reef complex was controlled by rising sea level and by local tectonism, leading to alternations of submergence and reefal exposure. While exposed, reef corals were neomorphosed and dissolved. When the corals were submerged, secondary porosity was filled by calcite cements precipitated from marine-derived waters. During the latest stages of reef development, rate of sea-level rise could no longer keep space with tectonic uplift and, while younger accretionary units continued to be deposited, older units were exposed subaerially, leading to the precipitation of meteoric calcite cement and to the development of a paleosol. This stage of diagenesis also affected the reef complex during late Kimmeridgian times, as the Boreal and Tethys coastlines progressively retreated to the north and southeast, respectively. Progressive retreat of the Boreal Sea and subsequent late Jurassic to early Cretaceous rifting that formed the Cameros Basin resulted in the deposition of Tithonian continental carbonates directly on these reefal units. Oxygen isotope compositions of these continental carbonates are 3‰ more negative than Kimmeridgian meteoric cement, suggesting an evolution in the isotopic composition of meteoric water in response to an increasing continental effect on meteoric precipitation.

In contrast, early Kimmeridgian reef complexes of the Torrecilla en Cameros Formation in the southern sectors of the seaway, closer to the Tethys Sea, were exposed

during the late Kimmeridgian as the Tethys coastline retreated, leading to dissolution of corals and subsequent precipitation of meteoric calcite cement. Oxygen isotope compositions of these meteoric cements are 2‰ more negative than time-equivalent meteoric calcites precipitated in the northern Torrecilla Reef Complex. Given the regional paleogeography, this difference suggests that sources of meteoric water must have been different for the northern and southern sectors, and probably reflects southward transport of air masses and water vapor from the Boreal Sea to the northern Torrecilla sector, and northwest transport of water vapor from the Tethys Sea to the southern sectors. Tithonian-Berriasian continental carbonates, which unconformably overlie reef complexes in the southern and northern sectors, exhibit an opposite trend, with the $\delta^{18}O$ of continental carbonates in southern sectors being 1.6‰ more positive than time-equivalent carbonates that overlie the Torrecilla Reef Complex to the north. This shift in the trend of the isotopes between northern and southern sectors is coeval with paleogeographic changes that occurred in response to late Jurassic-early Cretaceous rifting of the Iberian Plate and the progressive retreat of Boreal and Tethys coastlines. During this time, continental carbonates in both the southern and northern sectors of the seaway precipitated from meteoric waters that were sourced from the Tethys Sea to the southeast. More negative $\delta^{18}O$ values in the northern Torrecilla sector reflect enhanced continental fractionation effects as the influence of the Boreal Sea-derived meteoric waters diminished.

INTRODUCTION

Numerous studies have demonstrated the utility of $\delta^{18}O$ analysis for deciphering multiple stages of meteoric alteration in ancient carbonate successions (e.g., Dickson and Coleman 1980; Allan and Mathews 1982; Moldovanyi and Lohmann 1984; Lohmann 1987; Saller and Moore 1991; Frank and Lohmann 1995; Benito et al. 2001). Moreover, the application of $\delta^{18}O$ as a proxy for meteoric-water composition in an ancient regional paleogeographic context has the potential of greatly amplifying our understanding of the paleogeography and paleoclimate of a region (e.g., Hays and Grossman 1991; Ufnar et al. 2001; Ufnar et al. 2002).

In this study, we have employed a combination of sedimentologic, stratigraphic, petrologic, and geochemical observations to define the sequence and timing of alteration of a succession of early Kimmeridgian through Tithonian marine and nonmarine carbonates. This allows the dating of individual episodes of alteration, so that the $\delta^{18}O$ of meteoric calcites formed during local or regional exposure can be placed within a temporal and spatial context. As such, within a single stratigraphic succession, the progressive change in meteoric-water composition can be estimated from change in the $\delta^{18}O$ of the associated calcite cements which, in turn, might reflect an evolution in continental climate and/or aridity, or differences in source regions and storm tracks. Conversely, a regional comparison among temporally equivalent cements provides insights into the paleogeographic and paleoclimate regimes which give rise to isotopically distinct cement compositions. Factors controlling the $\delta^{18}O$ of these cements include orographic or "continental" effects (proximity to the ocean relative to storm tracks) and regional paleotemperatures. Analysis of $\delta^{18}O$ of cements within a sedimentologic and

paleogeographic context allows discrimination of the relative roles of each of these factors. For example, several studies have reconstructed the paleogeography of the Iberian Plate during the late Jurassic and early Cretaceous (e.g., Alonso and Mas 1990; Mas et al. 1993; Aurell and Meléndez 1993; Salas et al. 2001; Bádenas and Aurell 2001a) and have estimated the orientation of paleostorm tracks on the basis of sedimentologic criteria (e.g., Marsaglia and Klein 1983; Price et al. 1995; Bádenas and Aurell 2001b). The addition of cement $\delta^{18}O$ data as a proxy for changes in the isotopic composition of meteoric water can provide an independent test of such reconstructions. This study is such an examination of the North Iberian region during the early history of the Atlantic Ocean and evolution of the Boreal and Tethys seas.

GEOLOGIC SETTING

Tectonic and Depositional Framework

The study area is located in the northern part of the Iberian Range (Fig. 1), a positive tectonic element that developed in response to inversion of the Iberian Basin. The Iberian Basin formed during four major stages of extension (Álvaro et al. 1979; Vilas et al. 1983; Salas and Casas 1993; Roca et al. 1994; Salas et al. 2001): (1) Permo-Triassic rifting; (2) Jurassic post-rift subsidence; (3) late Jurassic-early Cretaceous rifting; and (4) late Cretaceous post-rift subsidence. This research focuses on the Kimmeridgian succession, the last episode of Jurassic post-rift sedimentation, which is represented by the coral reef complexes of the Torrecilla en Cameros Formation (Fig. 1B). The Torrecilla en Cameros Formation in the Cameros area has been dated as early Kimmeridgian (Benke et al. 1981; Conze et al. 1984; Errenst 1990, 1991), a period of rising global sea level (Vail et al. 1977; Vail et al. 1984; Haq et al. 1988), the effects of which are observed across the Iberian and northern Tethys domain (Alonso and Mas 1990; Aurell and Meléndez 1993,

Leinfelder 1993, 1994; Bádenas and Aurell 2001a).

Reefs of the Torrecilla en Cameros Formation were located along the western margin of an epicontinental seaway, the Soria Seaway (Bulard 1972), which was situated between the Iberian and the Ebro massifs and connected the Boreal realm, to the north, with the Tethys Sea, to the south (Fig. 1B). Reefs were best developed to the southeast (the Soria and Bigornia sectors) and near Torrecilla en Cameros, to the north (Fig. 1A, B). Geometry of the reef complexes was controlled by a prevailing rise in sea level during early Kimmeridgian, and by local basin tectonics. In the southern sectors, reef geometry was dominated by vertical and seaward accretion (Alonso and Mas 1990; Benito et al. 2001; Benito and Mas 2002), suggesting that despite the combination of positive eustasy and subsidence, high rates of carbonate production controlled overall reef growth. In contrast, in the northern Torrecilla sector, complexes developed as a series of offlapping reefs in response to local tectonism (Alonso et al. 1986-1987; Alonso and Mas 1990; Mas et al. 1997). Although this study is focused mainly on the Torrecilla Reef Complex (Fig. 1B, C), prior diagenetic analyses of reefs of the southern sector are included to provide a context for regional comparisons.

In late Kimmeridgian the Soria Seaway was bisected, with the Boreal and Tethys coastlines retreating to the north and southeast, respectively (Alonso and Mas 1990; Aurell and Meléndez 1993; Bádenas and Aurell 2001a) (Fig. 1B). Subsequently, in the Tithonian, deposition of marine sediments of the Torrecilla en Cameros Formation was replaced by a continental sedimentary regime in response to relative fall in sea level, and the rifting that led to the formation of the latest Jurassic and early Cretaceous Cameros continental basin (Salomon 1982; Guiraud and Seguret 1985; Mas et al. 1993; Aurell et al. 1994; Bádenas and Aurell 2001a; Salas et al. 2001) (Fig. 1). This rapidly subsiding continental basin was

filled during the Tithonian to middle Albian by up to 5000 m of fluvial and lacustrine sediments, with rare marine incursions (Mas et al. 1993). These continental sediments overlie the late Jurassic marine carbonates of the Torrecilla en Cameros Formation and are separated by an erosional unconformity with associated paleosols, hematitic crusts, and/or paleokarst features (Alonso and Mas 1990; Benito et al. 2001; Benito and Mas 2002). This unconformity is present throughout the region, in both the northern and southern sectors, and its development exerted a significant control on the meteoric alteration of the early Kimmeridgian reefal sequences (Benito et al. 2001; Benito and Mas 2002).

Sedimentology of the Torrecilla Reef Complex

The Torrecilla Reef Complex is located in the outskirts of the town of Torrecilla en Cameros (La Rioja, North Spain); (Fig. 1C). The succession exposed in this area is composed of a fringing reef complex including eight attached accretionary units that prograded towards the northeast (Fig. 2). Sedimentation of the first four units occurred in a rimmed shelf environment where reefs prograded as a stepped margin (Fig. 2). In contrast, the fifth and following units were deposited on a shallow platform where reefs grew in a shallow environment protected from waves and storms by longshore bars (Fig. 2).

The geometry and sedimentary evolution of the Torrecilla Reef Complex is consistent with deposition of reefs during relative sea-level fall (Alonso et al. 1986-1987; Alonso and Mas 1990; Mas et al. 1997). Given that the early Kimmeridgian was a time of rising sea level (e.g., Vail et al. 1977; Vail et al.1984; Haq et al. 1988; Bádenas and Aurell 2001a; Aurell et al. 2004), it is probable that the Torrecilla Reef Complex formed as a consequence of local tectonism that tilted and subsided the basin to the northeast, while the Variscan Demanda Block, which lies to the southwest, was

uplifted (Alonso et al. 1986-1987; Alonso and Mas 1990; Mas et al. 1997) (Fig. 1A, B). In this context, reef progradation was interrupted by periodic episodes of subaerial exposure induced by local tectonism. This continued until the rate of tectonic uplift exceeded the rate of eustatic sea-level rise. As a consequence, the proximal areas of the platform with the older accretionary units were then exposed and eroded, and the younger units were deposited in progressively shallower and more siliciclastic-rich environments (Fig. 2).

The top of the Torrecilla Reef Complex corresponds to a major unconformity developed in response to a global fall in sea level and the rifting that gave rise to the Cameros Basin during the latest Jurassic-early Cretaceous (Mas et al. 1993; Guimerá et al. 1995; Salas et al. 2001) (Fig. 1A). In this area, continental sedimentation of the Cameros Basin began with deposition of the Tithonian-age Ágreda Formation (Tera Group; Mas et al. 1993; Gómez-Fernández and Meléndez 1994) which consists of clays, conglomerates, sandstones, and lacustrine and palustrine limestones, and corresponds to the first depositional sequence (J10.1) of the basin (Salas et al. 2001; Arribas et al. 2003). The boundary between the reef complex and the continental unit is marked by an erosional surface with a well-developed paleosol (Fig. 3).

METHODS

This study is based on a detailed analysis of four stratigraphic sections (NR, National Road, OR, Old Road, TH, Tómalos Hermitage, RR, Ribabellosa Road), and several isolated outcrops (Fig. 1C). A total of 250 samples from these sections and isolated outcrops were then used for a petrographic, microsampling, and geochemical study of sedimentary and diagenetic features, utilizing standard petrographic techniques and cathodoluminescence, combined with an elemental and isotopic analysis of depositional and diagenetic carbonates. For each sample a polished and uncovered thin

section was prepared to 30 μm thickness. A matching thick section was also prepared with a thickness of 150-200 μm for microsampling of components for geochemical analysis. Cathodoluminescence (CL) examination was carried out using a Technosyn® cold cathodoluminescence unit. Following examination with CL, all thin sections were stained with Alizarin Red S and potassium ferricyanide (Dickson 1966). On the basis of petrographic observations, discrete depositional and diagenetic phases were microsampled from thick sections using a microscope-mounted drilling system available at the University of Michigan. Sample areas ranged from 300 to 500 μm in diameter resulting in 100-150 μg powdered carbonate samples.

Analyses for $\delta^{13}C$ and $\delta^{18}O$ were performed in the Stable Isotope Laboratory at the University of Michigan. Isotopic ratios are reported in per mil notation relative to the VPDB standard. Values were calibrated utilizing NBS 19 as the primary standard, and analytical precision was maintained at better than 0.1‰ for $\delta^{13}C$ and $\delta^{18}O$.

Elemental analyses for Ca, Mg, Sr, Mn, and Fe were performed on an electron microprobe. All analyses were conducted with an accelerating voltage of 15 kV and a spot size of 5 μm. Detection limits were 100 ppm for Mg, 250 ppm for Sr, 200 ppm for Mn, and 250 ppm for Fe. To allow direct comparison with isotopic analyses, all elemental analyses were made on the same thick sections.

Bulk mineralogy of the paleosol was analyzed by X-ray diffraction methods After removal of carbonate with acetic acid (Jackson 1969), an oriented aggregate of the < 20 μm fraction was obtained by sedimentation from an aqueous suspension. The sample was heated at 550ºC for 2 hours, and then was solvated with ethylene glycol at 65ºC over 48 h. Samples were analyzed on a Philips X-Ray difractometer, using Cu Kα radiation.

PETROGRAPHIC OBSERVATIONS OF THE TORRECILLA REEF COMPLEX

Information regarding synsedimentary and early meteoric processes is contained within the succession of diagenetic features and components present in the reefal limestones (Fig. 4), the unconformity-related paleosol, and lacustrine deposits of the Tithonian Ágreda Fm. (Fig. 3). These include early marine components that have been modified by marine, meteoric-marine, and meteoric waters.

The principal skeletal allochem is coral aragonite; corals constitute a significant component of the framework of the reef. The aragonite was mainly affected by dissolution, although many massive corals underwent neomorphic replacement represented by a porphyrotopic and xenotopic mosaic (*sensu* Friedman 1965) of nonferroan and low-magnesium calcite (LMC). Under CL, this calcite is nonluminescent (NL), or dark dull luminescent (DL) with small mottles of brightly luminescent (BL) calcite (Fig. 5A).

Most of the moldic porosity formed by dissolution of corals; secondary and primary porosity, not completely filled by micrite, was cemented by a nonferroan, NL or very dark DL bladed calcite cement that commonly forms isopachous layers up to 500 μm thick (Figs. 4A, 5A, B). Bladed calcite cement is more abundant and thicker in the lower and middle part of the sequence, where it may occlude pores up to 1 mm wide.

In the upper part of the sequence, where dissolution of branching and massive corals predominated, thickness of bladed calcite is lower (< 100 μm) and is commonly followed by a zoned NL/BL nonferroan to slightly ferroan drusy mosaic of calcite

cement up to 1500 μm thick (Figs. 4C, 5B). Bladed calcite is absent at the top of the sequence, as both primary and secondary pores are initially filled by a nonferroan and zoned NL/BL drusy mosaic of calcite cement up to 3 mm wide (Fig. 5C). This generation of NL/BL drusy calcite is absent or scarce and very thin (< 100 μm) in the lower to middle part of the section.

Bladed and drusy mosaic of calcite cements are postdated by late diagenetic cements (Fig. 5A-C) composed of DL ferroan calcite, and subsequent NL saddle ankerite that precipitated during burial of the reefal unit (Benito 2001). Ankerite, in turn, can be replaced by nonferroan cloudy calcite (BL to light DL) that contains iron oxides and hydroxides and relict inclusions of ankerite that precipitated during the Tertiary to present uplift-related diagenesis (Benito, 2001).

Paleosol Diagenetic Features at Torrecilla Reef Complex

The top of the Torrecilla en Cameros Formation was eroded and deeply weathered when it was exposed subaerially, and a paleosol developed prior to deposition of the Tithonian-age Ágreda Formation (Fig. 3). This paleosol consists of a heterogeneous horizon, up to 2 m thick, containing irregular fragments of reefal limestone embedded in a silty-sandy, yellowish carbonate matrix. The abundance of reefal fragments decreases relative to the matrix in the upper part of the paleosol, where the abundance of terrigenous material increases. Reefal fragments within the paleosol profile are brecciated and highly altered. In the upper part of the paleosol, these fragments are partially dissolved and/or replaced by pedogenic micritic calcite that forms nodules or breccia fragments in some places (Figs. 4D, 6A, B). Porosity that was present after this brecciation is cemented by a generation of nonferroan and NL/BL prismatic calcite (Figs. 4D, 6B). Rare calcite pseudomorphs after gypsum are present in association with pedogenic micrite (Fig. 6A). More commonly, locally this micrite can

be locally replaced by an equigranular and subidiotopic mosaic of calcite crystals, up to 30-40 μm wide, that typically show rhombohedral shapes (Figs. 4D, 6C). Calcite within these mosaics is nonferroan and NL, although the cores of some crystals consist of ferroan calcite or are dark and contain abundant iron oxide and hydroxide inclusions. Replacement and brecciation of reefal fragments continued, and siderite, berthierine, and hematite precipitated within the uppermost part of the paleosol (Figs. 4E, F; 6D, E, H). Siderite is very scarce and has been observed only with SEM as small crystals < 40 μm in vugs within pedogenic micrite and subidiotopic mosaics of calcite (Fig. 6D). Remaining porosity was partially or totally occluded by berthierine (a greenish and iron-rich trioctahedral clay mineral) and scattered quartz (Fig. 6D, E) that also postdates drusy mosaic of calcite cement precipitated within the reefal limestone at the top of the unit (Fig. 6E).

The uppermost part of the paleosol corresponds to an irregular-shaped and mottled, reddish-green layer of sandstone up to 30 cm thick (Fig. 3). Sandstone is largely replaced by berthierine, which, in turn, is partially replaced by hematite, particularly towards the top of the layer, which corresponds to an intensely nodularized and hematitic crust (Figs. 4F, 6F). Formation of nodules and precipitation of hematite is restricted to the top of the sandstone and is postdated by the deposition of overlying Tithonian continental deposits (Fig. 3). In the RR stratigraphic section (Fig. 1), however, below the ferruginous sandstone layer, an isolated sandy limestone, 60 cm thick, is present that contains gyrogonites of characea and abundant rhizoliths, at both a microscale and a mesoscale (Figs. 3B, 6G, H). Porosity in the sandy limestone is restricted to intraskeletal voids in characea and rhizoliths, and is mostly filled by kaolin (Fig. 6G).

Claystones, lacustrine limestones, conglomerates, and sandstones of the Tithonian-age Ágreda Formation overlie the hematitic crust of the paleosol in all the studied stratigraphic sections (Fig. 3). Lacustrine limestone (Fig. 7) is laminated, may contain up to 50-60% of silty to fine sandy quartz, ostracods, and plant fragments, and can be nodular, rippled, and/or burrowed. Early-formed porosity in these laminated limestones is restricted to small cracks, up to 1 mm thick, that are occasionally developed inside some micritic nodules. Cracks are partially filled by nonferroan and NL scalenohedral calcite cement, less than 100-150 μm thick, followed by micrite or a late diagenetic mosaic of cloudy calcite that contains inclusions of iron oxides and hydroxides.

GEOCHEMICAL RESULTS

Isotopic and trace-element compositions were determined for all diagenetic phases identified in this study. The elemental chemistry of these carbonate phases is summarized in Figure 8 and isotope values in Figures 8 and 9. A common feature noted for most diagenetic phases is that Sr and Mg contents are lower and $\delta^{13}C$ values more negative in samples collected from the upper part and top of the Torrecilla en Cameros Fm. compared to samples from the lower part (Figs. 8, 9).

Marine micrite matrix has low Sr content (up to 0.13 mole % $SrCO_3$), relatively high Mg content (from 0.19 to 2.24 mole % $MgCO_3$), variable Fe content (from 0 to 1.8 mole % $FeCO_3$), and low Mn (up to 0.1 mole % $MnCO_3$). Marine micrite has a wide range in both $\delta^{18}O$ and $\delta^{13}C$ values, and ranges from –2.1 to –6.9‰ in $\delta^{18}O$ and from +0.2 to –6.8‰ in $\delta^{13}C$.

Fibrous cement is rare. It is low in Sr content (from 0 to 0.11 mole % $SrCO_3$) and

is relatively high in Mg content (from 0.23 to 2.73 mole % $MgCO_3$). Fe and Mn are uniformly low (up to 0.11 and 0.17 mole %, respectively).

Neomorphic calcite replacing coral skeletons is also low in Sr content (up to 0.13 mole %) and high in Mg (from 0.56 to 2.5 mole %), whereas Fe and Mn contents are generally below detection. Neomorphic calcite yields values of 0 and +1.2‰ in $\delta^{13}C$, and –2.7 and –1.2‰ in $\delta^{18}O$, respectively, similar to those of bladed calcite, described below.

Bladed calcite cement has the highest Sr values (from 0 to 0.18 mole % $SrCO_3$), and the highest Mg content (from 0.32 to 3.86 mole % $MgCO_3$). Fe and Mn contents are low or below detection (up to 0.33 and 0.14 mole %, respectively). Bladed calcite defines a field of isotopic variation that ranges from –1.2 to –3.3‰ (mean value of –2.3‰) in $\delta^{18}O$, and from +2 to –1.2‰ in $\delta^{13}C$ (mean value of 0.9 ‰).

Drusy mosaic calcite that precipitated after bladed cements contains no measurable Sr, and relatively low Mg (generally less than 0.4 mole %, although values range up to 1.6 mole %). The luminescent character of these early phases of cement is controlled by variation in the Fe and Mn content; both concentrations are very low in the NL calcite (up to 0.3 and 0.05 mole %, respectively) but may increase to 0.5 mole % of Fe and 0.23 mole % of Mn in BL zones. No significant differences have been observed between elemental compositions of cement precipitated in the upper and lower parts of the unit. Nonferroan drusy calcite defines a field centered about –3.5‰ $\delta^{18}O$ and is marked by considerable variation in $\delta^{13}C$ ranging from –5.3 to –8.8‰ (Figs. 8-9).

An **echinoderm** fragment collected from the top of the reef complex has an isotopic value of –5.5‰ in $\delta^{13}C$ and –3.3‰ in $\delta^{18}O$, very similar to those of drusy mosaic calcite.

Elemental and isotopic compositions of carbonate phases associated with the paleosol of the top of the Torrecilla en Cameros Formation are:

Pedogenic micrite contains no measurable or very low Sr and Mn (up to 0.075 and 0.05 mole %, respectively), relatively high Mg content (up to 1.3 mole%), and variable Fe that ranges between 0.03 and 2.3 mole %.

Prismatic calcite that precipitated after brecciation of pedogenic micrite has no measurable or very low Sr (up to 0.06 mole %), relatively low Mg and Fe (up to 0.5 and 0.3 mole %, respectively), and very low (when NL) to low (in BL zones) Mn content (up to 0.02 and 0.1 mole %, respectively). Pedogenic micrite and prismatic calcite have isotopic values indistinguishable from drusy mosaic calcite: micrite has a value of –6.9‰ $\delta^{13}C$ and –4.4‰ $\delta^{18}O$, and prismatic calcite ranges from –7.3 to –8‰ $\delta^{13}C$ and from –3.5 to –4‰ $\delta^{18}O$.

Calcite in gypsum pseudomorphs has very low Sr (up to 0.06 mole %), low Mn, in general (up to 0.32 mole %) and relatively high Mg and Fe contents (up to 1 and 1.7 mole%, respectively). This calcite yields values of –4 to –4.3‰ $\delta^{13}C$ and –6.6 to –7‰ $\delta^{18}O$.

Subidiotopic mosaic of calcite occurring as replacement of pedogenic micrite has no to very low Sr content, up to 0.05 mole %, and relatively low Mg, Fe and Mn (up to 0.15, 0.17 and 0.06 mole %, respectively) where the calcite is NL, and relatively high Mg, Fe and Mn content (up to 1, 1.9 and 0.13 mole %, respectively) where the calcite is DL, as in the core of some of the crystals. Subidiotopic mosaics of calcite range from –5.1 to –5.6‰ $\delta^{13}C$ and from –6.9 to –7.1‰ $\delta^{18}O$.

Siderite has, in general, less than 0.04 mole % $SrCO_3$, although one of the samples has Sr content of 0.26 mole %, moderate Mn, up to 0.4 mole %, and relatively high Ca and Mg (up to 1.4 and 2.5 mole % respectively).

Carbonate powder from the **sandy limestone** deposited directly below the ferruginous sandstone at the RR section, and from the **laminated lacustrine limestone** of the Ágreda Fm. was also collected from thick sections. Early diagenetic meteoric carbonate cements coeval with sedimentation of these deposits are very scarce or too thin to be microsampled with accuracy, thus discrete areas of micrite lacking evidence of neomorphic replacement or other diagenetic alteration were used to characterize meteoric conditions present during deposition of this lacustrine sequence. Whole-rock isotopic analysis has been demonstrated as a viable approach to identify intervals of subaerial exposure, to determine the diagenetic processes active during development of paleosols, and in climatic studies based on micritic lacustrine deposits (e.g., Allan and Matthews 1982; Goldstein 1991; Drummond et al. 1996). In our case, both petrographic and geochemical observations argue against subsequent diagenetic alteration of these deposits. Carbonate micrite of both deposits have less than 0.05 mole % $SrCO_3$, moderate Mg and Fe, up to 0.4 and 0.5 mole %, respectively, and less than 0.1 mole % $MnCO_3$ (Fig. 8). Sandy limestone yields isotopic values of –6.5 to –7.8‰ $\delta^{13}C$ and –6.6 to –6.7‰ $\delta^{18}O$, and laminated lacustrine limestones range between –6.9 and –7‰ $\delta^{18}O$, and –4.2 and –4.4‰ $\delta^{13}C$. This combination of elemental and isotopic data argue for deposition and diagenesis in a meteoric setting (Allan and Matthews 1982; Lohmann 1987). Sr, Mg, and Fe contents are low, and the isotopic data define a trend with invariant $\delta^{18}O$ and variable $\delta^{13}C$ values (Fig. 9). Moreover, $\delta^{13}C$ values are more negative in the sandy limestone, where soil features are more abundant, than in laminated limestones, where they are scarce or even absent.

In addition, calcite in gypsum pseudomorphs, subidiotopic calcite, sandy limestones, and laminated lacustrine limestones of the Ágreda Formation define a field of values centered about –6.8‰ in $\delta^{18}O$ with $\delta^{13}C$ varying from –4 to –7.8‰.

TIMING OF EARLY DIAGENETIC EVENTS OF THE TORRECILLA REEF COMPLEX

Petrographic observations and geochemical analyses suggest that at least four distinctive diagenetic stages affected the Torrecilla Reef Complex during deposition and development of the unconformity, and prior to the burial of the unit. This diagenetic evolution was controlled mainly by the eustatic and tectonic history of the area, which led to an alternation of subaerial exposure and submergence during the early Kimmeridgian and prolonged exposure of reefs in the late Kimmeridgian, prior to burial by continental sediments since the Tithonian. To establish the starting composition of the marine assemblage prior to alteration by diagenetic fluids, we have compiled data on Jurassic belemnites and oysters by Veizer et al. (1999) and abiotic marine cements (Lohmann 1987) for the Kimmeridgian (Fig. 9).

Stage 1 - Early Kimmeridgian This stage, coeval with sedimentation of the reefal sequence, was characterized by early marine phreatic diagenesis that includes micritization and precipitation of micrite and fibrous calcite in primary pores (Fig. 4A). These marine carbonates, originally formed as high-magnesium calcite and/or aragonite, were subsequently neomorphosed, as suggested by textural features and by elemental and isotopic data that deviate from the primary marine values (Figs. 5A, 9). Moreover, isotopic data on marine micrite show a broad range of values in both $\delta^{13}C$ and $\delta^{18}O$,

which, in the case of $\delta^{18}O$, are similar to later diagenetic calcite cements, suggesting that marine micrite was subsequently altered during later stages of meteoric diagenesis.

Stage 2 - Early Kimmeridgian. This stage is characterized by an alternation of meteoric- and marine-related diagenesis that occurred prior to the definitive subaerial exposure of the reefal sequence, and led to neomorphism and dissolution of coral skeletons and precipitation of bladed calcite within both primary and moldic pores (Fig. 4B).

Geochemical features of bladed cement and calcite from neomorphosed coral skeletons suggest a marine-related origin. They contain relatively high Sr and Mg contents, and most isotopic values are included in the field defined for the isotopic composition of Kimmeridgian marine carbonate, and approach the isotopic composition inferred for Kimmeridgian abiotic cements (Lohmann 1987; Veizer et al. 1999); (Figs. 8, 9). Bladed calcite precipitated not only in primary but also in secondary moldic pores. This observation indicates that dissolution of coral aragonite occurred prior to or contemporaneous with cementation. Considering that the evolution of Torrecilla Reef Complex was controlled by local tectonic uplift combined with a eustatic sea-level rise (Alonso et al. 1986-1987; Alonso and Mas 1990; Mas et al. 1997), dissolution of corals could have occurred when reefs were episodically exposed, and bladed calcite precipitation when reefs were subsequently submerged.

Stage 3 – Post-marine, early Kimmeridgian sedimentation and pre-Tithonian continental sedimentation: This stage was characterized by prolonged exposure of reefs and subsequent development of paleosol. The age of this sequence is constrained by the sedimentologic relationships. First, during the deposition of late stages of reef accretion, older accrectionary units of the Torrecilla Reef complex were already subaerially exposed while younger accretionary units were still depositing (Fig. 2). Second, the entire reefal

sequence is overlain by Tithonian-age continental deposits of the Ágreda Fm. On this basis, it is probable that this stage is latest early Kimmeridgian through late Kimmeridgian in age.

During this period of exposure, the drusy mosaic of calcite cement precipitated after dissolution and neomorphism of corals and emplacement of bladed calcite (Figs. 4C, 5B, C). Petrographic and geochemical features of this cement (see Dickson and Coleman 1980; Brand and Veizer 1980; Lohmann 1987; James and Choquette 1990) strongly suggest precipitation in a meteoric phreatic environment. It consists of nonferroan calcite with very low Sr and Mg content, and isotopic compositions significantly more negative than marine values. Isotopic data define a field characterized by relatively invariant $\delta^{18}O$ and variable and negative $\delta^{13}C$ values (Fig. 9), a trend that is indicative of a water-dominated diagenetic system with an input of soil-derived, isotopically light carbon (Lohmann 1987). Neomorphism of marine carbonates (as micrite, and fibrous calcite) by meteoric waters likely occurred during this stage, leading to higher incorporation of light carbon from soils and less incorporation of Sr and Mg in calcites in the uppermost part of the unit, proximal to the subaerial exposure surface.

Pedogenic micrite and nonferroan prismatic calcite that precipitated as intergranular cement between breccia fragments have Sr and Mg contents and isotopic compositions very similar to those of the drusy mosaic calcite cement (Fig. 9). Thus, it is probable that all these phases precipitated within the same meteoric diagenetic system. Subidiotopic mosaics of calcite (Fig. 4D, 6C) with rhombohedral shapes that locally replaced pedogenic micrite are interpreted as early dedolomitization of an earlier formed dolomite that likely developed in association with gypsum (Evamy 1967; Purser 1985; Arenas et al. 1999). Isotopic compositions of dedolomite and calcite in gypsum pseudomorphs are similar, however, but they are distinct from meteoric diagenetic

carbonates discussed above (Fig. 9). Although dolomite and gypsum were precipitated during this stage, dedolomitization and replacement of gypsum by calcite must have occurred at a later stage under different environmental conditions and in equilibrium with geochemically distinct waters.

Stage 4 - Tithonian. During this stage, sandy limestones, containing characea and abundant rhizoliths, and sandstone, were deposited in small, shallow ponds. The $\delta^{13}C$ and $\delta^{18}O$ variation present in the sandy limestone suggests precipitation in a meteoric environment; but the $\delta^{18}O$ values are approximately 3.3‰ more negative than meteoric carbonates precipitated during Stage 3 (Fig. 9), suggesting that they precipitated at a time when environmental conditions had changed and/or the composition of meteoric water was distinctly different.

Following deposition of sandy limestone and sandstone, siderite and berthierine precipitated (Figs. 4E, 6D, E). These minerals are interpreted to precipitate from fresh to brackish waters, in suboxic conditions with low sulfate content, during the earlier stages of diagenesis in coastal floodplains and in association with laterites (Coleman 1985; Curtis and Coleman, 1986; Taylor and Curtis 1995; Hornibrook and Longstaffe 1996; Mackay and Longstaffe 1997; Fritz and Toth 1997; Toth and Fritz 1997). The restriction of these minerals to the uppermost part of the paleosol and to sandy limestones and sandstones, and the absence of associated sulfides (e.g., pyrite), suggest formation under similar environmental conditions, after deposition of the sandy limestones and sandstones in the Torrecilla area. Notably, after deposition, nodules were formed in the sandstones, and bertheriene, carbonate, and quartz were replaced by hematite (Figs. 4F, 6H), suggesting a transition from suboxic conditions to a more oxidizing environment that is requisite for hematite precipitation.

Given that the sedimentological and geochemical features of these deposits (Figs. 8, 9) are very similar to those of the laminated lacustrine limestones of the Ágreda Fm. (see below), it is probable that deposition of sandy limestones and sandstones and the development of nodules and the hematitic crust occurred during the first stages of the Tithonian Ágreda Fm. sedimentation, rather than representing prior diagenetic alteration related to exposure of the reefal unit in latest early to late Kimmeridgian.

Stage 5 - Tithonian. Clays, sandstones, conglomerates, and lacustrine and palustrine limestones of the Tithonian Ágreda Formation were deposited after development of the hematite-rich paleosol (Gómez-Fernández and Meléndez 1994). The laminated limestones at the base of this formation, the sandy limestone, and calcite replacement of dolomite and gypsum all exhibit similar isotopic values, suggesting that their formation is intimately related to a common process of meteoric alteration.

SPATIAL AND TEMPORAL EVOLUTION OF THE $\delta^{18}O$ VALUES OF METEORIC CARBONATES: PALEOGEOGRAPHIC AND PALEOCLIMATIC IMPLICATIONS

Herein, we first provide a comparison of meteoric carbonates from early Kimmeridgian successions in the northern sector of Torrecilla with those of the southern sector at Soria and Bigornia. We examine differences in isotopic composition in a spatial context that relate to the regional paleogeography. We then examine the succession of carbonate chemistries within individual localities to evaluate temporal change during meteoric diagenesis in order to elucidate long-term patterns of paleogeography. In this fashion, comparison of meteoric calcite $\delta^{18}O$ in a temporal and spatial context has the potential to elucidate the evolution of regional climate.

I. Spatial Trends in $\delta^{18}O$ of Kimmeridgian Meteoric Cements:

During Kimmeridgian/Tithonian, the Iberian Plate was located between 20º and 30º N (Moore et al. 1992; Price et al. 1995; Weissert and Mohr 1996) and mean surface temperatures ranged between 15 and 25ºC (Valdes and Sellwood 1992; Moore et al. 1992). Prior research that focused on patterns of sedimentation of the Iberian Basin during Kimmeridgian times provides reconstructions of the regional paleogeography and estimates the directions of paleostorm tracks (e.g., Alonso and Mas 1990; Aurell et al. 1994; Bádenas and Aurell 2001a, 2001b). It has been suggested that Kimmeridgian hurricanes, generated in the Tethys area (Fig. 10), produced storms that moved to the northwest (Marsaglia and Klein 1983), and winter storms that moved east-southeast (Price et al. 1995). The direction of these storm tracks is supported by the orientation of ramps that developed preferentially on the windward side of the Iberian Basin (Bádenas 1999; Bádenas and Aurell 2001b). Therefore, if depletion of Kimmeridgian meteoric precipitation occurred in response to a continental effect, one would expect the most positive $\delta^{18}O$ values for meteoric waters in the southern sectors of the Soria Seaway (closer to the source region of the Tethys Sea) and more negative $\delta^{18}O$ values in northern Torrecilla sector, a trend opposite to that observed in the data (Figs. 10, 11A)

Reefal complexes of the southern region (Soria and Bigornia sectors) were subaerially exposed and altered by meteoric waters during the late Kimmeridgian in response to the retreat southeast of the Tethys coastline (Aurell et al. 1994; Mas et al. 1997; Benito et al. 2001; Bádenas and Aurell 2001a; Benito and Mas 2002) (Fig. 10). The northern Torrecilla Reef Complex was also completely exposed in late Kimmeridgian in response to the retreat of the Boreal coastline to the north (Mas et al. 1997; Bádenas and Aurell 2001a) (Figs. 1B, 10). The older accretionary units of the Torrecilla Reef Complex were exposed due to local tectonism in the latest early Kimmeridgian while deposition of younger reefs continued (Alonso et al. 1986-1987; Mas et al. 1997) (Fig. 2). Thus, it is

probable that precipitation of meteoric cements was not strictly coeval in northern and southern sectors, in as much as meteoric precipitation would have begun earlier in the northern sector (in the older accretionary units of the Torrecilla Reef complex). The $\delta^{18}O$ of meteoric calcite precipitated in both the older and the younger accretionary units of the Torrecilla Reef Complex is quite similar and still distinct from cements formed in the southern sector. For example, in samples where meteoric calcite cements are thick enough for more than one analysis to be performed (as in the sample of Figure 5C), differences are smaller than 0.5‰ $\delta^{18}O$ and 1‰ $\delta^{13}C$ in all the cases. These data suggest that the meteoric diagenetic system did not change significantly throughout the time that the Torrecilla Reef complex was exposed (from the latest early Kimmeridgian to the late Kimmeridgian). Thus, the latest early to late Kimmeridgian meteoric calcite cements of the Torrecilla Reef Complex can reasonably be considered approximately coeval and comparable to late Kimmeridgian meteoric cements precipitated in southern sectors.

While the isotopic compositions of meteoric calcites in southern sectors are very similar, lying along a meteoric calcite line at –5.5‰ $\delta^{18}O$, at Torrecilla area the $\delta^{18}O$ values of latest early to late Kimmeridgian meteoric calcites are distinctly different (Fig. 11A), with an offset of approximately +2‰. It is unlikely that the offset in isotopes between southern and northern sectors is due to differences in the water-rock interaction, because the data do not fit a carbon and oxygen isotopic trend characteristic of this process (Lohmann 1987; Meyers and Lohmann 1985). Thus, the observed offset in $\delta^{18}O$ values must reflect regional differences in either environmental conditions (i.e., temperature and/or aridity) or primary differences in the isotopic composition of the meteoric precipitation.

If one assumes that the isotopic compositions of meteoric precipitation were the same between the northern and southern sectors, the observed +2‰ offset at Torrecilla

could result from a surface temperature that was colder by 9-10°C (Friedman and O'Neil 1977). Given the low elevation of the Iberian Basin during this time period and the limited geographical distance between the study areas (< 100 km) (Fig. 10), such large changes in temperature are unlikely.

On the contrary, if we assume constant surface temperature during each time interval, the observed offset in isotope composition of meteoric calcite would be controlled mainly by variation in groundwater $\delta^{18}O$. Differences in groundwater $\delta^{18}O$ could result from increased surface evaporation. In order to effect a +2‰ shift in water composition at Torrecilla, assuming Rayleigh fractionation of surface waters (Bottinga and Craig 1969), an increase of 20% surface evaporation would be necessary. There are several observations that argue against this possibility: If evaporation or aridity were significant enough to effect a +2 ‰ shift in $\delta^{18}O$ of meteoric cements in the Torrecilla area, one could expect the most positive $\delta^{18}O$ values in samples collected from the upper part of the reefal unit and the paleosol, because evaporation preferentially removes ^{16}O from porewaters at the air-sediment interface (Allan and Matthews 1982). In fact, this is the case of the southern Soria sector, where late Kimmeridgian meteoric calcites present in the uppermost meter of the reefal sequence yield mean $\delta^{18}O$ values 0.9‰ more positive than elsewhere in the sequence (Benito and Mas 2002). In contrast, in the northern Torrecilla sector, no significant differences are observed in $\delta^{18}O$ values of drusy meteoric calcites precipitated from either the base or the top of the reefal sequence (Fig. 9). Similarly, differences in isotopic values (less than 0.5‰ $\delta^{18}O$ and 1‰ $\delta^{13}C$) have not been found when analyses of sucessive cements were performed, suggesting that the environmental conditions were very similar throughout the time that meteoric calcites were precipitated. The only difference is observed in $\delta^{13}C$ values, which, as expected, are more negative in meteoric calcites precipitated at the top of the unit (Fig. 9).

Pedogenic micrite and prismatic calcite precipitated after brecciation of micrite, formed during late stages of reefal exposure and soil development (Figs. 4C, D, 6A), yield $\delta^{18}O$ values similar to those of the meteoric drusy calcite cement present in the reefal sequence. The rare occurrence of dolomite and gypsum in the pedogenic micrite suggests ephemeral conditions of aridity during the early stages of exposure. It is likely that the dolomite and gypsum, and the meteoric calcite phases, did not precipitate simultaneously. Rather, dolomite and gypsum could have precipitated during a period of relatively arid conditions, whereas the meteoric calcite cements and pedogenic micrite formed during more persistent stages of higher humidity.

In contrast to primary differences in regional temperature or aridity, it is possible that the $\delta^{18}O$ composition of meteoric precipitation during the late Kimmeridgian may have varied regionally, with the southern sectors being more negative relative to the northern region of Torrecilla. Such geographically controlled differences can be produced by a "continental effect" resulting in a progressive landward decrease in $\delta^{18}O$ of meteoric precipitation in response to Rayleigh fractionation of atmospheric water vapor along the direction of storm tracks. Such patterns are observed today across the Iberian Peninsula (Plata 1994), with progressively more negative $\delta^{18}O$ precipitation with increasing distance inland from the coastlines. Even in areas of low elevation, changes of 2 to 3‰ are common. The observed pattern of less negative values, however, in the northern sector would require that the dominant storm tracks were from north to south. This is contrary to sedimentologic evidence and palaeoclimate reconstructions, which indicate dominant northward movement of storms initiated in the Tethys Sea (Marsaglia and Klein 1983; Price et al. 1995; Bádenas and Aurell 2001b). Thus, our observations suggest separate marine source regions for meteoric waters. The northern sector at

Torrecilla may have derived its precipitation from the Boreal Sea, whereas waters derived from the Tethys Sea to the southeast dominated in the southern sector (Fig. 10).

The Iberian Plate was located between 20º and 30º N (Moore et al. 1992; Price et al. 1995; Weissert and Mohr 1996), and the mean surface temperatures of the Iberian Plate during Kimmeridgian and Tithonian times ranged approximately between 15 and 25°C (Valdes and Sellwood.1992; Moore et al. 1992), for which an average groundwater temperature of 20°C would be reasonable. Thus, on the basis of $\delta^{18}O$ values of meteoric calcites and assuming a 20°C groundwater temperature, water isotopic values at northern Torrecilla sector would have been about –2.5‰ VSMOW (Friedman and O'Neil 1977), a value quite plausible given the proximity of the Boreal coastline and the low to mid-latitude of the Iberian Basin in late Jurassic (Hays and Grossman 1991, Bowen and Wilkinson 2002). Similarly, the isotopic composition of meteoric carbonates in the southern region, at both Soria and Bigornia sectors, would require meteoric groundwaters of approximately –4 to –4.5‰ VSMOW (at 20°C). Given little evidence of differences in temperature or evaporation between these two regions, or differences in the isotopic composition of the Boreal and Tethyan Seas, the more negative values observed in the southern sector imply a more pronounced continental effect. In effect, the negative values observed at Soria and Bigornia require a greater distance from the coastline of the Tethyan Sea than the Boreal coastline that affected the Torrecilla region, reflecting a more extensive retreat of the Tethys Sea during this time. Thus, the isotopic composition of meteoric carbonate may serve as a valuable constraint for defining the position of the late Kimmeridgian coastlines. Specifically, paleogeographic reconstructions have previously situated the Boreal shoreline farther to the north (Bádenas 1999; Bádenas and Aurell 2001a) (Fig. 10)

because of the lack of available stratigraphic data below the Ebro Basin Tertiary sediments (Fig. 1).

II. Temporal Trends in $\delta^{18}O$ of Kimmeridgian and Tithonian Meteoric Carbonates

During the Tithonian, several paleogeographic changes within the Iberian Plate occurred as a consequence of the progressive retreat of the Tethys and Boreal seas (Fig. 9), and the late Jurassic-early Cretaceous rifting that led to formation of several sub-basins (i.e., the Cameros Basin and the western Basque-Cantabrian Basins) that were subsequently filled by continental sediments during the Tithonian-Berriasian (Alonso and Mas 1990; Aurell et al. 1994; Gómez-Fernández and Meléndez 1994; Bádenas and Aurell 2001a; Salas et al. 2001). In addition, during this time, western Europe underwent a slight climatic cooling and an increase in aridity (Hallam et al. 1991; Hallam 1993; Schudack 1999), changes that have been recorded in Tithonian meteoric cements from reefal carbonates at the Bigornia sector (Benito et al. 2001). Here we compare isotopic values of meteoric carbonates along the northern and southern sectors of the Soria Seaway and evaluate the role of paleogeography on temporal and spatial changes that have occurred in the composition of meteoric precipitation.

In the northern sector at Torrecilla, $\delta^{18}O$ values of Tithonian continental carbonates are about 3.3‰ more negative than the values of earlier precipitated Kimmeridgian meteoric cements (Figs. 9, 11B). If the shift had occurred as a consequence of a change in temperature (assuming no change in the $\delta^{18}O$ of meteoric water), calcite compositions would have required a temperature increase of 15ºC. Such a change is unreasonable considering that slight cooling and increased evaporation have been inferred for western Europe during this time period (Hallam et al. 1991; Hallam 1993; Schudack 1999). Cooling and/or evaporation would have resulted in an overall

enrichment in carbonate $\delta^{18}O$, a trend opposite to that observed in the calcite record. It is more reasonable that the observed difference in the $\delta^{18}O$ values reflects primary changes in the isotopic composition of meteoric water by 3-3.5‰ VSMOW (Friedman and O'Neil 1977). This scenario is possible given that, during the Tithonian, the Boreal coastline was farther north, as it was progressively retreating, and continental sediments were being deposited to the north in the Cameros and western Basque-Cantabrian basins, leading to an increased continental effect that would have resulted in a greater depletion of meteoric precipitation.

The $\delta^{18}O$ trend observed in the southern sectors, however, does not exhibit a temporal offset of this magnitude or direction. Kimmeridgian meteoric cements are very similar to those of Tithonian (or Tithonian-Berriasian in the Bigornia sector) continental carbonates (Benito et al. 2001; Benito and Mas 2002) (Fig. 11B). More critically, the $\delta^{18}O$ of southern sector continental carbonates are 1.6‰ more positive than coeval lacustrine carbonates that overlie the Torrecilla Reef Complex (Fig. 11B). This trend is the opposite of that observed for Kimmeridgian meteoric cements. If we consider changes in the paleogeography of the Iberian Plate during the Tithonian, it is possible that the source of meteoric waters shifted to the Tethys Sea exclusively, in as much as much of the northern Iberian Plate was exposed as large continental basins, and the position of the Boreal coastline was located much farther to the north (Fig. 10). In such a scenario, hurricanes and winter storms formed in the Tethys could generate storm tracks that moved from the southeast and south to provide meteoric precipitation for both the northern and southern sectors. Increased fractionation of meteoric precipitation along these storm tracks, in combination with a slightly cooling climate, could have produced isotopic values that are relatively unchanged in the southern sector, proximal

to the Tethys source, in comparison to the more negative values observed northward at Torrecilla.

ACKNOWLEDGMENTS

Funds for this study were provided by the Ministerio de Educación y Cultura of Spanish government (projects No. PB97-0298, BTE2001-026 and BTE2002-04453-C02-02). The authors would like to thank B.H. Wilkinson and L. Wingate, who improved this manuscript with their suggestions and comments, and to L. Wingate, G. Herrero, B. Moral, A. Fernández, and I. Sevillano for their technical support. We also thank R.H. Goldstein, D. Ulmer-Scholle, and B. Railsback for their careful and thoughtful reviews, which have significantly improved this paper, and R.H. Goldstein and J.B. Southard for their excellent editorial work.

REFERENCES

Allan, J.R., and Matthews, R.K., 1982, Isotope signatures associated with early meteoric diagenesis: Sedimentology, v. 29, p. 797-817.

Alonso, A., and Mas, R., 1990, El Jurásico superior marino en el Sector de la Demanda-Cameros (La Rioja-Soria), *in* Arche, A., ed., Estratigrafía del Jurásico de la Península Ibérica II: Cuadernos de Geología Ibérica, v. 14, p. 173-198.

Alonso, A., Mas, J.R., and Meléndez, N., 1986-1987, Los arrecifes coralinos del Malm en la Sierra de los Cameros (La Rioja, España): Acta Geológica Hispánica, v. 21-22, p. 296-306.

Álvaro, M., Capote, R., and Vegas, R., 1979, Un modelo de evolución tectónica para la cadena celtibérica: Acta Geológica Hispánica, v. 14, p. 172-177.

Arenas, C., Alonso-Zarza, A.M., and Pardo, G., 1999, Dedolomitization and other early diagenetic processes in Miocene lacustrine deposits, Ebro Basin (Spain): Sedimentary Geology, v. 125, p. 23-45.

Arribas, J., Alonso, A., Mas, R., Tortosa, A., Rodas, M., Barrenechea, J.F., Alonso-Azcárate, J., and Artigas, R., 2003, Sandstone petrography of continental depositional sequences of and intraplate rift basin: Western Cameros Basin (North Spain): Journal of Sedimentary Research, v. 73, p. 309-327.

Aurell, M., and Meléndez, A., 1993, Sedimentary evolution and sequence stratigraphy of the Upper Jurassic in central Iberian Chain, northeast Spain, *in* Posamentier, H.W., Summerhayes, C.P., Haq, B.U., and Allen, G.P., eds., Sequence stratigraphy and Facies Associations: International Association of Sedimentologists. Special Publication 18, p. 343-368.

Aurell, M., Mas, R., Meléndez, A., and Salas, R., 1994, El tránsito Jurásico-Cretácico en la Cordillera Ibérica: relación tectónica-sedimentación y evolución paleogeográfica: Cuadernos de Geología Ibérica, v. 18, p. 369-396.

Aurell, M., Robles, S., Bádenas, B., Rosales, I., Quesada, S., Meléndez, G., and García-Ramos, J.C., 2004, Transgressive-regressive cycles and Jurassic palaeogeography of northeast Iberia: Sedimentary Geology, v. 162, p. 239-271.

Bádenas, B., 1999, La sedimentación de las rampas carbonatadas del Kimmeridgiense en las cuencas del este de la Placa Ibérica: PhD. Thesis, Universidad de Zaragoza, 256 p.

Bádenas, B., and Aurell, M., 2001a, Kimmeridgian palaeogeography and basin evolution of northeastern Iberia: Palaeogeography, Palaeoclimatology, Palaeoecology, v. 168, p. 291-310.

Bádenas, B., and Aurell, M., 2001b, Proximal-distal facies relationships and sedimentary processes in a storm dominated carbonate ramp (Kimmeridgian, northwest of the Iberian Ranges, Spain): Sedimentary Geology, v. 139, p. 319-340.

Benito, M.I., 2001, Estudio comparativo de la evolución sedimentaria y diagenética de los litosomas carbonatados arrecifales (pre-rifting) de la Cuenca de Cameros. Kimmeridgiense. La Rioja-Soria: PhD Thesis, Universidad Complutense de Madrid, 410 p.

Benito, M.I., and Mas, R., 2002, Evolución diagenética de los carbonatos arrecifales de la Formación Torrecilla en Cameros y de los carbonatos continentales suprayacentes (Kimmeridgiense inferior-Titónico) en el Sector de Soria. Cuenca de Cameros, N. España: Journal of Iberian Geology, v. 28, p. 65-92.

Benito, M.I., Lohmann, K.C., and Mas, J.R., 2001, Discrimination of multiple episodes of meteoric diagenesis in a Kimmeridgian reefal complex, North Iberian Basin, Spain: Journal of Sedimentary Research, v. 71, p. 381-393.

Benke, K., Dürkoop, A., Errenst, C. and Mensink, H., 1981, Die Korallenkalke im Ober-Jura der nordwestlichen Iberischen Ketten (Spanien): Facies, v. 4, p. 27-94.

Bottinga, Y., and Craig, H., 1969, Oxygen isotope fractionation between CO_2 and water and the isotopic composition of marine atmospheric CO_2: Earth and Planetary Science Letters v. 5, p. 285-295.

Bowen, G.J., and Wilkinson, B.H., 2002, Spatial distribution of $\delta^{18}O$ in meteoric precipitation: Geology, v. 30, p. 315-318.

Brand, U., and Veizer, J., 1980, Chemical diagenesis of multicomponent carbonate system-I: Trace elements: Journal of Sedimentary Petrology, v. 50, p. 1219-1236.

Bulard, P.F., 1972, Le Jurassique Moyen et Supérieur de la Chaîne Ibérique sur la bordure du bassin de l'Ebre (Espagne): PhD Thesis, University of Nice, 2 vol., 702 p. Unpublished.

Coleman, M.L., 1985, Geochemistry of diagenetic non-silicate minerals: kinetic considerations: Royal Society (London), Philosophical Transactions, v. A315, p. 39-56.

Conze, R., Errenst, C., and Mensink, H., 1984, Die Ammoniten des Ober-Callovium bis Unter-Kimmeridgium in den Nordwestlichen Keltiberischen Ketten: Palaeontographica, A, v. 183, p. 162-211.

Curtis, C.D., and Coleman, M.L., 1986, Controls on the precipitation of early diagenetic calcite, dolomite and siderite concretions in complex depositional sequences. *in* Gautier, D.L., ed., Roles of Organic Matter in Sediment Diagenesis: SEPM, Special Publication 38, p. 23-34.

Dickson, J.A.D., 1966, Carbonate identification and genesis as revealed by staining: Journal of Sedimentary Petrology, v. 36, p. 491-505.

Dickson, J.A.D., and Coleman, M.L., 1980, Changes in carbon and oxygen isotope composition during limestone diagenesis: Sedimentology, v. 27, p. 107-118.

Drummond, C.N., Wilkinson, B.H., and Lohmann, K.C., 1996, Climatic control of fluvial-lacustrine ciclycity in the Cretaceous Cordilleran Foreland Basin, western United States: Sedimentology, v. 43, p. 677-689.

Errenst, C., 1990, Das korallenführende Kimmeridgium der nordwestlichen Iberischen Ketten und angrenzender gebiete (Fazies, paläogeographie und beschreibung der korallenfauna). Teil 1: Palaeontographica, A, v. 214, p. 121-207.

Errenst, C., 1991, Das korallenführende Kimmeridgium der nordwestlichen Iberischen Ketten und angrenzender gebiete (Fazies, paläogeographie und beschreibung der korallenfauna). Teil 2: Palaeontographica, A, v. 215, p. 1-42.

Evamy, B.D., 1967, Dedolomitization and the development of rombohedral pores in limestones: Journal of Sedimentary Petrology, v. 37, p. 1204-1215.

Frank, T.D., and Lohmann, K.C., 1995, Early cementation during marine-meteoric fluid mixing: Mississippian Lake Valley Formation, New Mexico: Journal of Sedimentary Research, v. A65, p. 263-273.

Friedman, G.M., 1965, Terminology of crystallization textures and fabrics in sedimentary rocks: Journal of Sedimentary Petrology, v. 35, p. 379-398.

Friedman, I., and O'Neil, J.R., 1977, Compilation of stable isotope fractionation factors of geochemical interest, *in* Data of Geochemistry. US Geological Survey, Professional Paper 440-KK, p. 1-12.

Fritz, S.J., and Toth, A.T., 1997, An Fe-Berthierine from a Cretaceous laterite: Part II. Estimation of Eh, pH and pCO_2 conditions of formation: Clays and Clay Minerals, v. 45, p. 580-586.

Goldstein, R.H., 1991, Stable isotopic signatures associated with palaeosols, Pennsylvanian Holder Formation, New Mexico: Sedimentology, v. 38, p. 67-77.

Gómez Fernández, J.C. and Meléndez, N., 1994, Estratigrafía de la "Cuenca de Cameros" (Cordillera Ibérica Noroccidental, N de España) durante el tránsito

Jurásico-Cretácico: Revista Sociedad Geológica de España, v. 7 (1-2), p. 121-139.

Guimerá, J., Alonso, A., and Mas, J.R., 1995, Inversion of an extensional-ramp basin by a neoformed thrust: The Cameros basin (N. Spain), *in* Buchanan, J.C., and Buchanan, P., eds., Basin inversion: Geological Society of London, Special Publication 88, p. 433-453.

Guiraud, M, and Seguret, M., 1985, A releasing solitary overstep model for the Late Jurassic-Early Cretaceous (Wealdian) Soria atrike-slip Basin (Northern Spain), *in* Biddle, K.T., and Christie-Blick, N., eds., Strike Slip Deformation. Basin Formation, and Sedimentation: SEPM, Special Publication 37, p. 159-175.

Haq, B.U., Hardenbol, J., and Vail, P.R., 1988, Mesozoic and Cenozoic chronostratigraphy and cycles of sea-level change, *in* Wilgus, C.K., Hastings, B.S., Kendall, C.G. St.C., Posamentier, H.W., Ross, C.A., and Van Wagoner, J.C., eds., Sea-Level Changes – An Integrated Approach: SEPM, Special Publication 42, 71-108.

Hallam, A., Grose, J.A., and Ruffell, A.H., 1991, Palaeoclimatic significance of changes in clay mineralogy across the Jurassic-Cretaceous boundary in England and France: Palaeogeography, Palaeoclimatology, Palaeoecology, v. 81, p. 173-187.

Hallam, A., 1993, Jurassic climates as inferred from the sedimentary and fossil record: Royal Society (London), Philosophical Transactions, v. B341, p. 287-296.

Hays, P.D., and Grossman, E.L., 1991, Oxygen isotopes in meteoric calcite cements as indicators of continental palaeoclimate: Geology, v. 19, p. 441-444.

Hornibrook, E.R.C., and Longstaffe, F.J., 1996, Berthierine from the Lower Cretaceous Clearwater Formation, Alberta, Canada: Clays and Clay Minerals, v. 44, p. 1-21.

Jackson, M.L., 1969, Soil chemical analysis: Advanced Course: a manual of methods useful for instruction and research in soil chemistry, physical chemistry of soils, soil fertility, and soil genesis Advanced Course, Second Edition: Madison, Wisconsin, 895 p.

James, N.P., and Choquette, P.W., 1990, Limestones – The meteoric diagenetic environment, *in* McIlreath, I.A., and Morrow, D.W., eds., Diagenesis: Geoscience Canada, Reprint Series 4, p. 35-73.

Leinfelder, R.R., 1993, Upper Jurassic Reef Types and controlling factors. A preliminary report: Profil, v. 5, p. 1-45.

Leinfelder, R.R., 1994, Distribution of Jurassic Reef Types: A mirror of structural and environmental changes during breakup of Pangea, *in* Beauchamp, B., Embry, A.F., and Glass, D., eds., Pangea: Global Environments and Resources: Canadian Society of Petroleum Geologists, Memoir 17, p. 677-700.

Lohmann, K.C., 1987, Geochemical patterns of meteoric diagenetic systems and their application to studies of palaeokarst, *in* James, N.P., and Choquette, P.W., eds., Palaeokarst: Berlin, Springer-Verlag, p. 58-80.

Mackay, J.L., and Longstaffe, F.J., 1997, Diagenesis of the Lower Cretaceous Clearwater Formation, Primrose Area, Northeastern Alberta, *in* Pemberton, S.G., and James, D.P., eds., Petroleum Geology of the Cretaceous Mannville Group, Western Canada: Canadian Society of Petroleum Geologists, Memoir 18, p. 392-412.

Marsaglia, K.M., and Klein, G.D., 1983, The paleogeography of Paleozoic and Mesozoic storm depositional systems: Journal of Geology, v. 91, p. 117-142.

Mas, J.R., Alonso, A., and Guimerá, J., 1993, Evolución tectonosedimentaria de una cuenca extensional intraplaca: la cuenca finijurásica-eocretácica de Los Cameros (La Rioja-Soria): Revista de la Sociedad Geológica de España, v. 6 (3-4), p. 129-144.

Mas, J.R., Alonso, A., and Benito, M.I., 1997, Depositional and diagenetic evolution of late Jurassic coral reefs in northern Iberian Ranges (North Spain): Boletín de la Real Sociedad Española de Historia Natural, Sección Geología, v. 92 (1-4), p. 143-160.

Meyers, W.J., Lohmann, K.C., 1985. Isotope geochemistry of regionally extensive calcite cement zones and marine components, *in* Schneidermann, N., and Harris, P.M., eds., Carbonate Cements: SEPM, Special Publication 36, p. 223-239.

Moldovanyi, E.P., and Lohmann, K.C., 1984, Isotopic and petrographic record of phreatic diagenesis: Lower Cretaceous Sligo and Cupido Formations: Journal of Sedimentary Petrology, v. 54, p. 972-985.

Moore, G.T., Hayashida, D.N., Ross, C.A., and Jacobson, S.R., 1992, Palaeoclimate of the Kimmeridgian/Tithonian (Late Jurassic) world: I. Results using a general circulation model: Palaeogeography, Palaeoclimatology, Palaeoecology, v. 93, p. 113-150

Plata, A., 1994, Composición isotópica de las precipitaciones y aguas subterráneas de la Península Ibérica: Madrid, Ministerio de Obras Públicas y Transportes, Centro de Estudios y Experimentación de Obras Públicas, 140 p.

Price, G.D., Sellwood, B.W., and Valdes P.J., 1995, Sedimentological evaluation of general circulation model simulations for the "greenhouse" Earth: Cretaceous

and Jurassic case studies: Sedimentary Geology, v. 100, p. 159-180

Purser, B.H., 1985, Dedolomite porosity and reservoir properties of Middle Jurassic carbonates in the Paris Basin, France, *in* Roehhl, P.D., and Choquette, P.W., eds., Carbonate Petroleum Reservoirs: Berlin, Spinger, p. 341-356.

Roca, E., Guimerá, J., and Salas, R., 1994, Mesozoic extensional tectonics in the southeast Iberian Chain: Geological Magazine, v. 131, p. 155-168.

Salas, R., and Casas, A., 1993, Mesozoic extensional tectonics, stratigraphy and crustal evolution during the Alpine cycle of the eastern Iberian basin: Tectonophysics, v. 228, p. 33-55.

Salas, R., Guimerá, J., Mas, R., Martín-Closas, C., Meléndez, A., and Alonso, A., 2001, Evolution of the Mesozoic Central Iberian Rift System and its Cainozoic inversion (Iberian Chain), *in* Ziegler, P., Cavazza, W., Roberston, A.H.F., and, Crasquin-Soleau, S., eds., Peri-Tethyan Rift/Wrench Basins and Passive Margins: Muséum National d'Histoire Naturelle, Mémoires 186, p. 145-185.

Saller, A.H., and Moore, C.H., Jr., 1991. Geochemistry of meteoric calcite cements in some Pleistocene limestones: Sedimentology, v. 38, p. 601-621.

Salomon, J., 1982, El Cretácico inferior Cap. 7. Cameros-Castilla, *in* Arche, A., ed., El Cretácico de España: Universidad Complutense de Madrid, p. 345-387.

Schudack, M.E., 1999, Ostracoda (marine/nonmarine) and palaeoclimate history in the Upper Jurassic of Central Europe and North America: Marine Micropalaeontology, v. 37, p. 273-288.

Taylor, K.G., and Curtis, D., 1995, Stability and facies association of early diagenetic mineral assemblages: an example from a Jurassic ironstone-mudstone succession, U.K: Journal of Sedimentary Research, v. 65, p. 297-310

Toth, T.A., and Fritz, S.J., 1997, An Fe-Berthierine from a Cretaceous laterite: Part I. Characterization: Clays and Clay minerals, v. 45, p. 564-579.

Ufnar, D.F., González, L.A., Ludvigson, G.A., Brenner, R.L., and Witzke, B.J., 2001, Stratigraphic implications of meteoric sphaerosiderite $\delta^{18}O$ values in paleosols of the Cretaceous (Albian) Boulder Creek Formation, NE British Columbia foothills, Canada: Journal of Sedimentary Research, v. 71, p. 1017-1028.

Ufnar, D.F., González, L.A., Ludvigson, G.A. Brenner, R.L., and Witzke, B.J , 2002, The mid-cretaceous water bearer: Isotope mass balance quantification of the Albian hydrologic cycle: Palaeogeography, Palaeoclimatology, Palaeoecology, v. 188, p. 51-71.

Vail, P.R., Hardenbol, J., and Todd, R.G., 1984, Jurassic unconformities, chronostratigraphy and sea-level changes from seismic stratigraphy and biostratigraphy, *in* Schlee, J.S., Ed., Interregional Unconformities and Hydrocarbon Accumulation: American Association of Petroleum Geologists, Memoir 36, p. 129-144.

Vail, P.R., Mitchum, R.M., Jr., Todd, R.G., Widmier, J.M., Thompson, S., III, Sangree, J.B., Bubb, J.N., and Hatlelid, W.G., 1977, Seismic stratigraphy and global changes of sea-level, *in* Payton, C.E., Ed., Seismic Stratigraphy – Applications to Hydrocarnbon Exploration: American Association of Petroleum Geologists, Memoir 26, p. 49-212.

Valdes, P.J., and Sellwood, B.W., 1992, A palaeoclimate model for the Kimmeridgian: Palaeogeography, Palaeoclimatology, Palaeoecology, v. 95, p. 47-72.

Veizer, J., Ala, D., Azmy, K, Bruckschen, J., Buhl, D., Bruhn, F., Carden, G.A.F., Diener, A., Ebneth, S., Godderis, Y., Jasper, T., Korte, C., Pawellek, F.,

Podlaha, O.G., and Strauss, H., 1999, $^{87}Sr/^{86}Sr$, $\delta^{13}C$ and $\delta^{18}O$ evolution of Phanerozoic seawater: Chemical Geology, v. 161, p. 68-88.

Vilas, L., Alonso, A., Arias, C., García, A., Mas, J.R., Rincón, R., and Meléndez, N., 1983, The Cretaceous of the Southwestern Iberian Ranges (Spain): Zitteliana, v. 10, p. 245-254.

Weissert, H., and Mohr, H., 1996, Late Jurassic climate and its impact on carbon cycling: Palaeogeography, Palaeoclimatology, Palaeoecology, v. 122, p. 27-43.

FIGURES

Fig.1. Location and geological maps. **A)** Outcrop location of the marine Jurassic deposits (black) around the North Iberian Basin (the Cameros Basin). **B)** Palaeogeography of the northern Iberian Peninsula during late Jurassic times. Early Kimmeridgian reef complexes are located in two regions: **1**. Northern region; **2**. Southern region. Early Kimmeridgian coastline is based on Alonso and Mas (1990) and Bádenas and Aurell (2001a). Possible location of late Kimmeridgian and Tithonian coastlines are based on Aurell et al. (1994), and Bádenas and Aurell (2001a). **C)** Geological map of the study area showing the locations of the four stratigraphic sections and isolated outcrops.

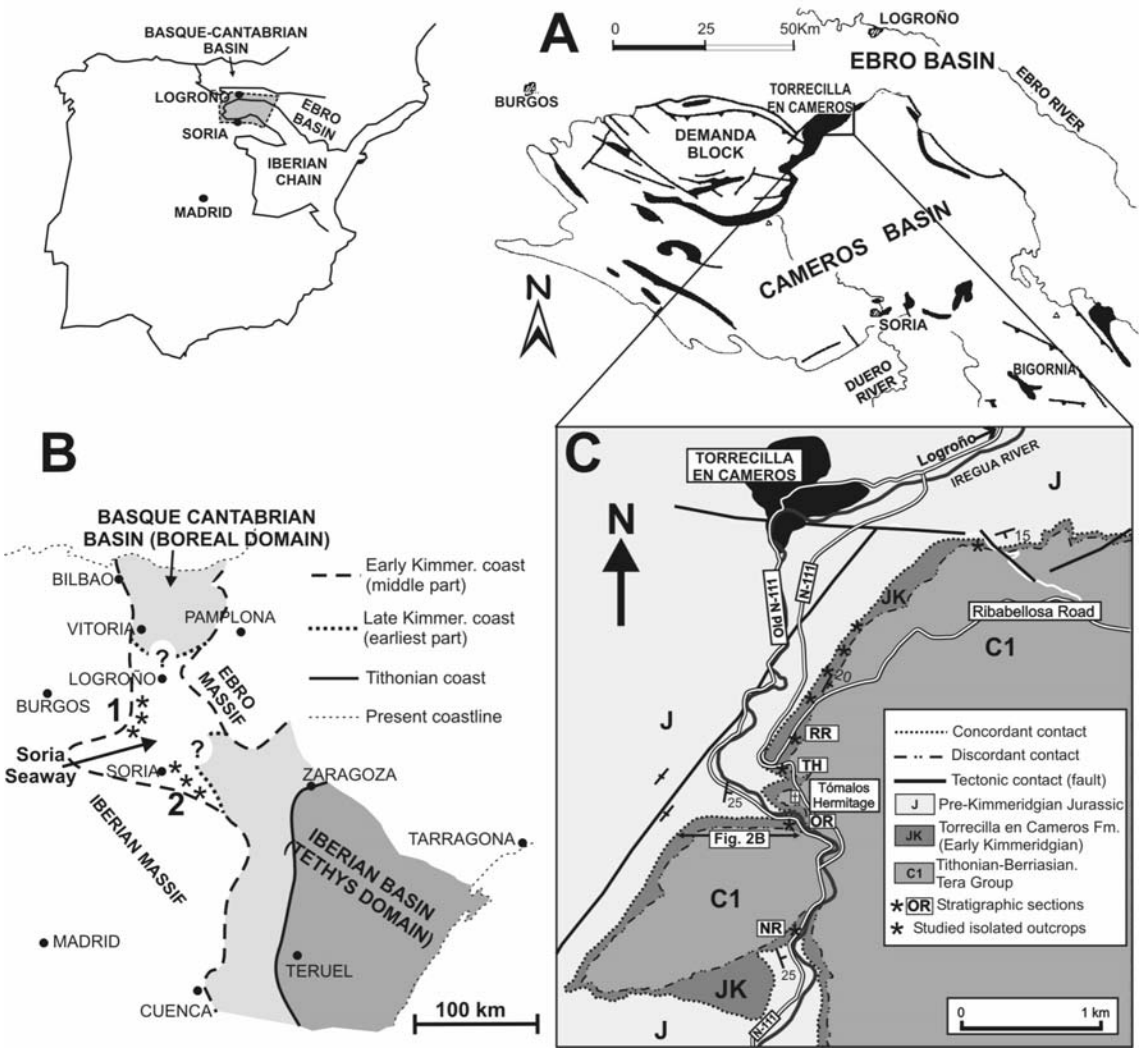

Fig. 2. Summary sketch illustrating the depositional geometry of the Torrecilla reef complex (see text for explanation). Light gray and black arrows indicate tectonic uplift and sea-level rise, respectively.

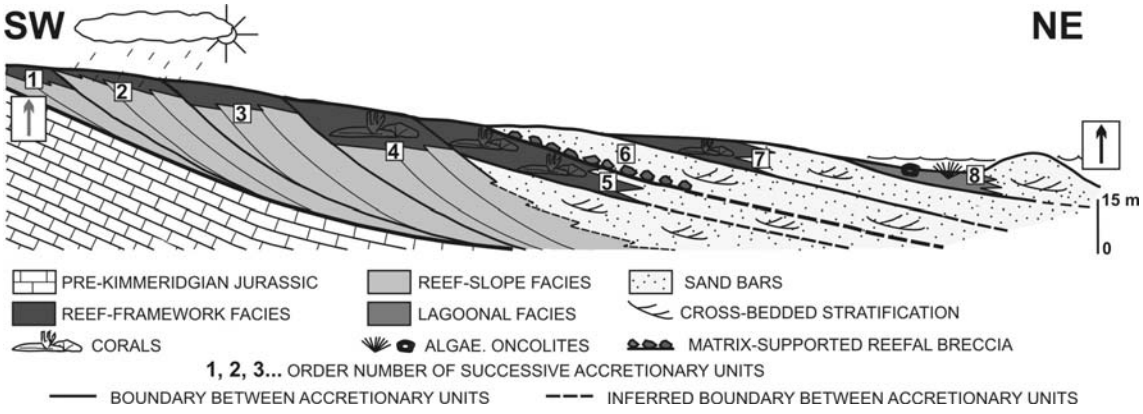

Fig. 3. Paleosol developed on top of the Torrecilla Reef Complex: **A)** TH section; **B)** RR section (see Fig. 1C for location).

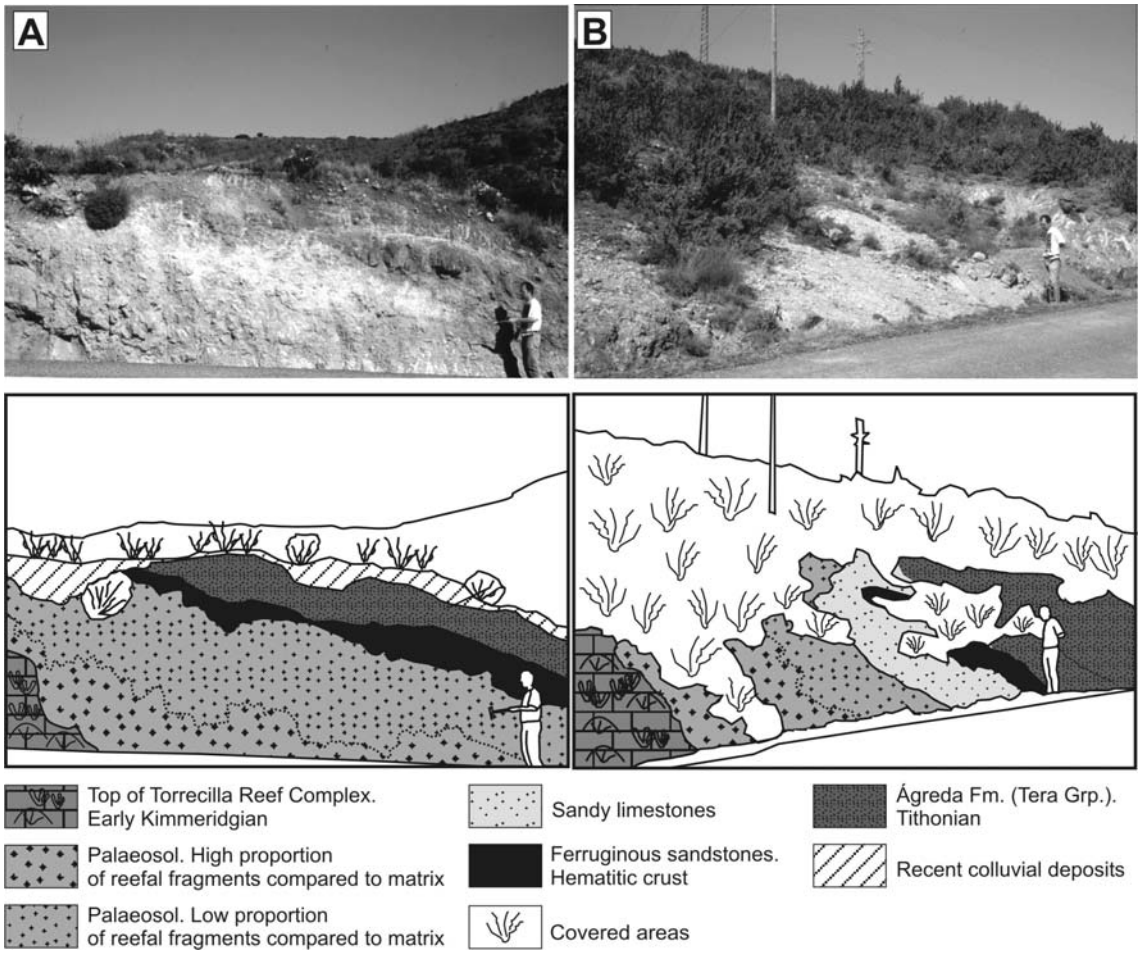

Fig. 4. Idealized sketches illustrating the paragenetic sequence of early diagenetic phases and events within the Torrecilla Reef Complex.

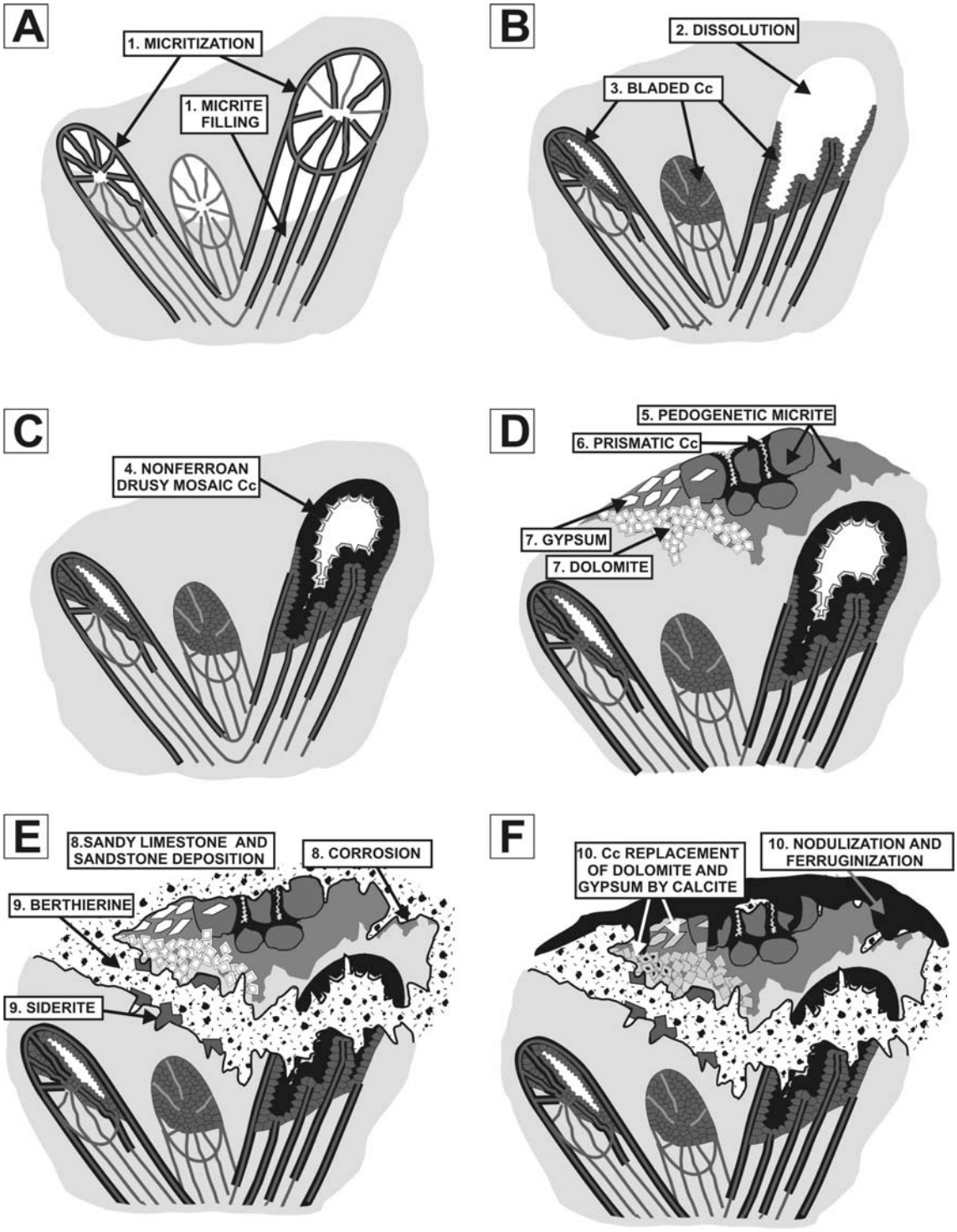

Fig. 5. A) Cathodoluminescence (CL) photograph of partially dissolved massive coral with voids cemented by nonluminescent bladed calcite (CC) and followed by a dully

luminescent ferroan calcite (FC). The neomorphosed coral is indicated by NC, which is a dully to brightly luminescent calcite. **B)** CL photograph showing primary porosity first cemented by a generation of NL bladed calcite (BC), which is followed by a nonferroan NL-BL drusy mosaic of calcite (MC). Remaining porosity is filled by a DL ferroan calcite (FC). **C)** CL photograph of a branching coral completely dissolved, with moldic pores cemented by a nonferroan and zoned NL-BL drusy mosaic of calcite (MC), and followed by DL ferroan calcite (FC).

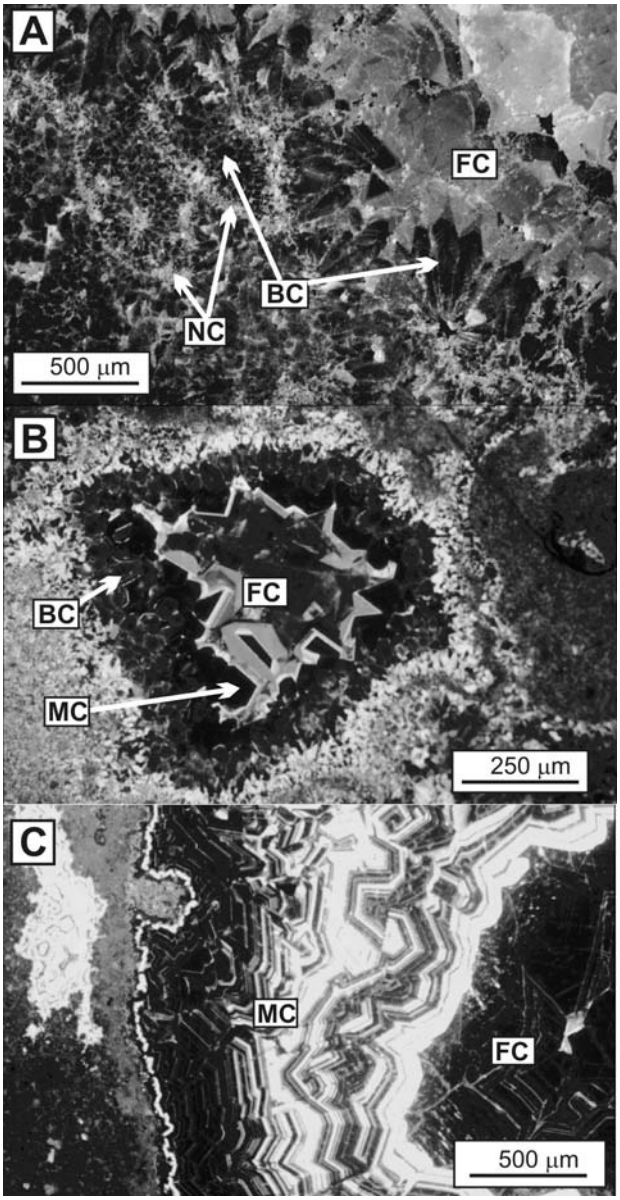

Fig. 6. **A)** Nodular micrite precipitated in the paleosol. Note the calcite pseudomorph after gypsum (Y) that is included in a nodule. **B)** CL photograph of brecciated pedogenic micrite (BM). Porosity is filled by nonferroan and NL-BL prismatic calcite (PC). **C)** Subidiotopic mosaic of calcite raplacing pedogenic micrite. Note the dark core of crystals and the rhombohedral shape. **D)** Vuggy porosity after nodulization and brecciation of pedogenic micrite, filled by siderite (S), berthierine and quartz (B+Q). **E)** Vuggy porosity affecting reefal limestone (RL) at the top of the complex, which is cemented by drusy calcite (MC) and later by berthierine (B). **F)** Root marks present in sandy limestones deposited below ferruginous sandstones at RR section (see Fig. 3B). Lens cap for scale. **G)** Detail of the sandy limestone. Porosity inside characea and rhizoliths is filled by kaolin. **H)** Nodules formed in ferruginous sandstone at the top of the paleosol exhibit circumgranular cracking and are largely replaced by hematite.

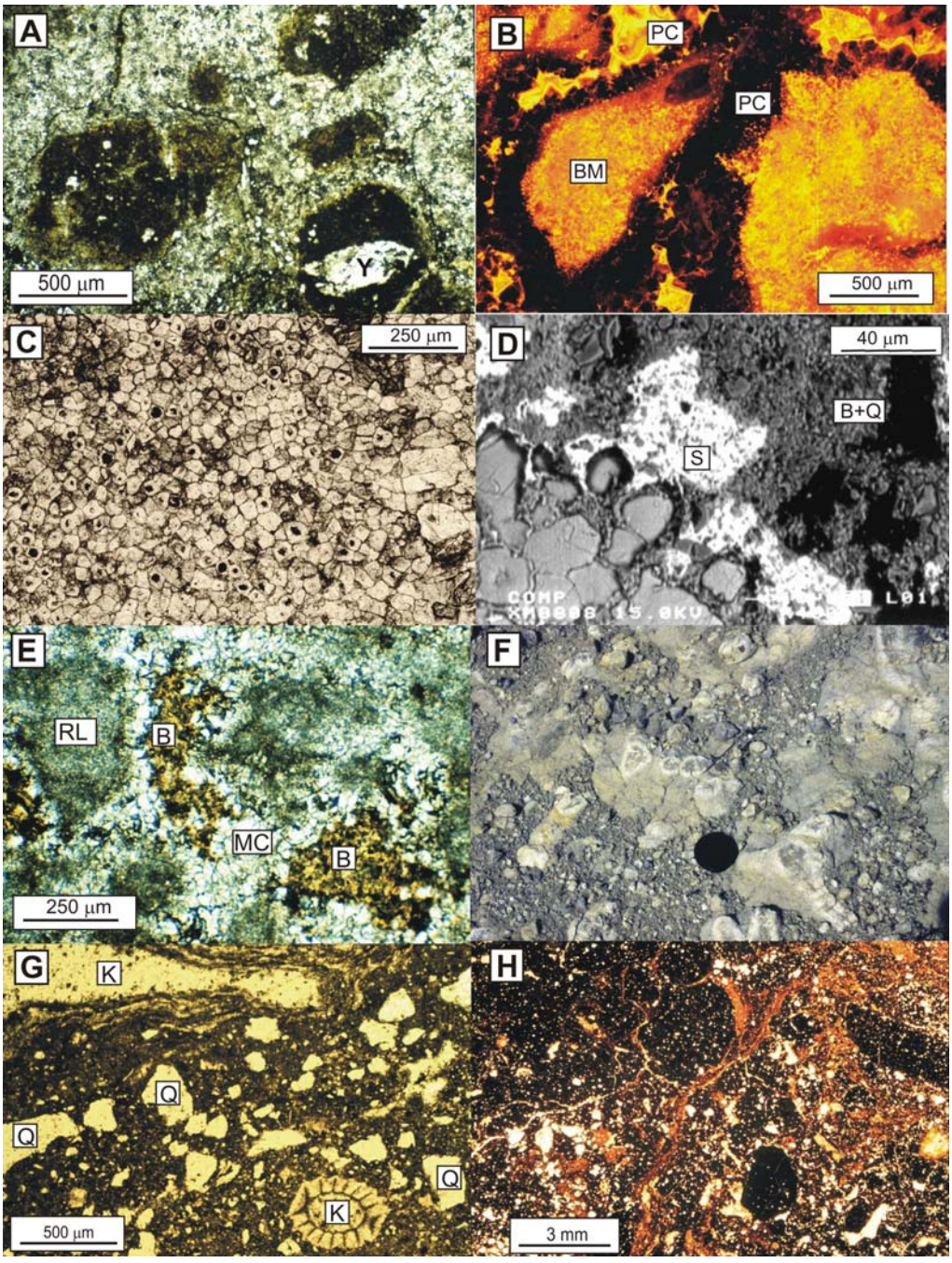

Fig. 7. Detailed photograph of the Tithonian lacustrine limestones of the Ágreda Fm.

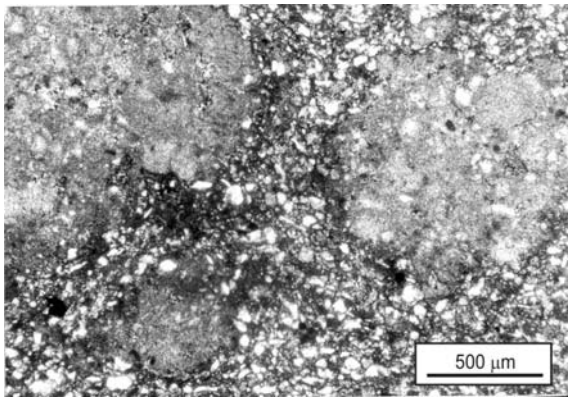

Fig. 8. Summary of elemental and isotopic chemistry of diagenetic phases, and the inferred ages and diagenetic environments associated with each paragenetic element (see the discussion section for explanation). Minor-element compositions are expressed in $MeCO_3$ mole %. Detection limits are indicated by vertical lines, labeled Dl. The observed ranges in elemental compositions are illustrated by horizontal black bars, with the mean values as white vertical bars. Mean values that are below detection limit are omitted. NL, nonluminescent; BL, brightly luminescent; DL, dully luminescent. N is the number of elemental analyses; n is the number of isotopic analyses. Expanded scale for Sr and Mn.

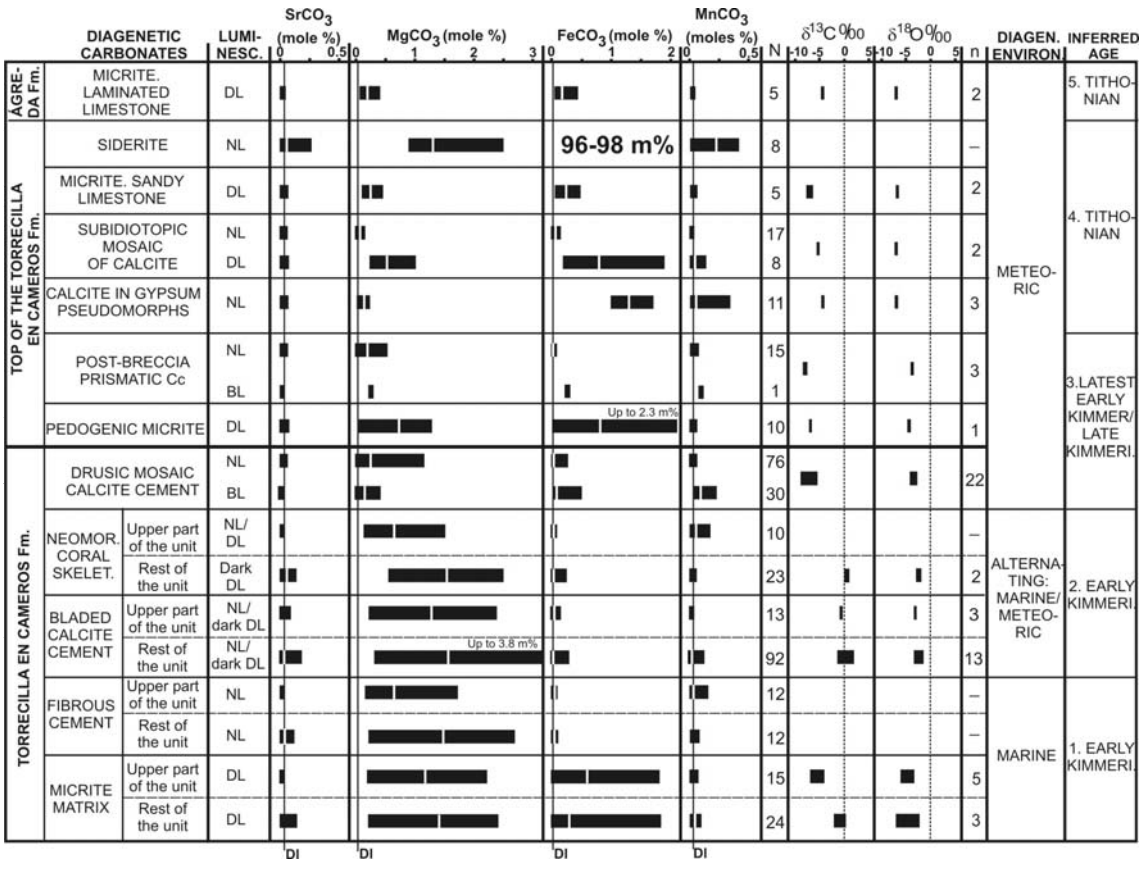

Fig. 10. Paleogeography of northeastern Iberian Plate and inferred coastlines for Boreal and Tethys seas during the Kimmeridgian and Tithonian. Tracks of hurricanes and winter storms for the late Jurassic are based on Marsaglia and Klein (1983), Price et al. (1995), and Bádenas and Aurell (2001b). Early Kimmeridgian coastline is based on Alonso and Mas (1990) and Bádenas and Aurell (2001a); Tithonian coastline is based on Aurell et al. (1994) and Bádenas and Aurell (2001a).

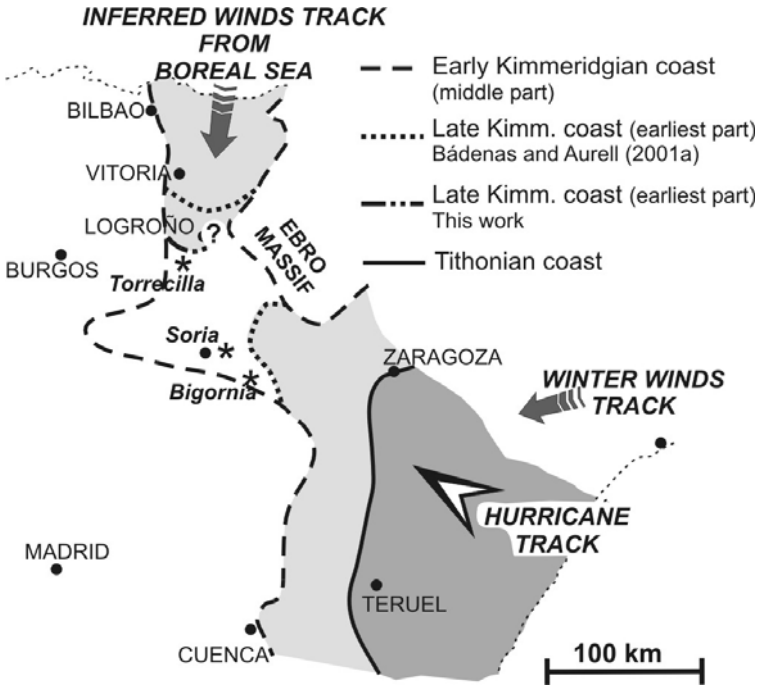

Fig. 11. Comparison between isotopic compositions of meteoric carbonates precipitated in the northern region at the Torrecilla Reef Complex and the southern region (comprising Soria and Bigornia sectors) (see Fig. 1A and B for locations). Isotopic data of meteoric calcites precipitated in the Soria and Bigornia sectors are based on Benito and Mas (2002) and Benito et al. (2001), respectively. **A)** Kimmeridgian cements. **B)** Tithonian to Tithonian-Berriasian meteoric carbonates. Dotted-line ellipses correspond to meteoric cements precipitated during the Kimmeridgian, shown in part A.